JOURNAL OF MATERIALS SCIENCE **39** (2004) 5311–5314

Evolution of textures and microstructures in IF-steel sheets during continuous confined strip shearing and subsequent recrystallization annealing

Y. H. JIN, M. Y. HUH
Division of Materials Science and Engineering, Korea University, Seoul 136-701, Korea

Y. H. CHUNG*
Advance Metals Research Center, Korea Institute of Science and Engineering, P.O. Box 131, Cheongryang, Seoul 130-136, Korea
E-mail: yhchung@kist.re.kr

Interstitial free (IF) steel sheets were deformed by continuous confined strip shearing (CCSS) based on the equal channel angular pressing (ECAP). The samples were deformed by CCSS up to three passages and subsequently recrystallized at 700°C for 1 h. The strain history of IF steel sheets in the CCSS die-channel was tackled by finite element method (FEM) simulations. The deformation by CCSS led to the shear deformation and consequently the formation of shear texture components. With increasing number of CCSS passages, the intensity of the deformation texture was hardly increased. The recrystallization texture resembled the deformation texture. The orientation stability was discussed by mean of Taylor deformation model and the formation of recrystallization textures was discussed by occurrence of the discontinuous recrystallization. Observations by transmission electron microscopy (TEM) and electron backscattered diffraction (EBSD) revealed the formation of ultra-fine grains in IF sheets deformed by CCSS.

1. Introduction

Ultrafine-grained (UFG) bulk materials have attracted great research interest because the mechanical and physical properties distinguish UFG materials from conventional coarse-grained materials, e.g. [1]. Severe plastic deformation has become a popular method for processing UFG microstructures. Equal channel angular pressing (ECAP) is now one of the most common methods to impose severe plastic deformation to rod-shaped bulk materials, e.g. [2].

Recently, we have proposed the novel method of "continuous confined strip shearing" (CCSS) which, based on ECAP, provides repeated shear deformation on strip metals, e.g. [3–5]. Likewise ECAP, the thickness of the strips is preserved during CCSS forming. In addition, as in ordinary rolling, the CCSS process enables continuous operation of metallic strips by utilizing a set of the feeding roll and the guide roll (Fig. 1). Recent works on several aluminum alloys demonstrated that UFG are successfully produced by CCSS and subsequent annealing [4–6].

Interstitial free (IF) steel shows favorable high planar anisotropy and is widely used in the manufacturing of panels for automobiles. Because the carbon and nitrogen atoms in solution of IF steel are scavenged as titanium and/or niobium containing precipitates, IF steel exhibits commonly low strength [7]. Strengthening by grain refinement is beneficial since UFG metallic materials tend to have high strength without sacrificing ductility. In the present work, the CCSS process was applied to IF steel in order to track the impact of repeated shear deformation by CCSS on the evolution of texture and microstructure. Furthermore, the recrystallization in IF steel deformed by CCSS was also studied.

2. Experimental procedure

IF steel (0.002% C, 0.01% Si, 0.09% Mn, 0.0014% P, 0.009% S, 0.0042% Al, 0.053% Ti) used in this study was supplied by POSCO, Korea. The as-received material was 1.0 mm thick, cold rolled and fully recrystallized IF steel sheet. This initial material was used for CCSS. As shown in Fig. 1, the tools of the CCSS operation were designed to provide a constant shear strain by feeding the strip through an equal channel angular (ECA) channel with an angle Φ of 120° and a curvature Ψ of 0°. The feeding speed into the ECA channel was controlled through the radial velocity of the

*Author to whom all correspondence should be addressed.

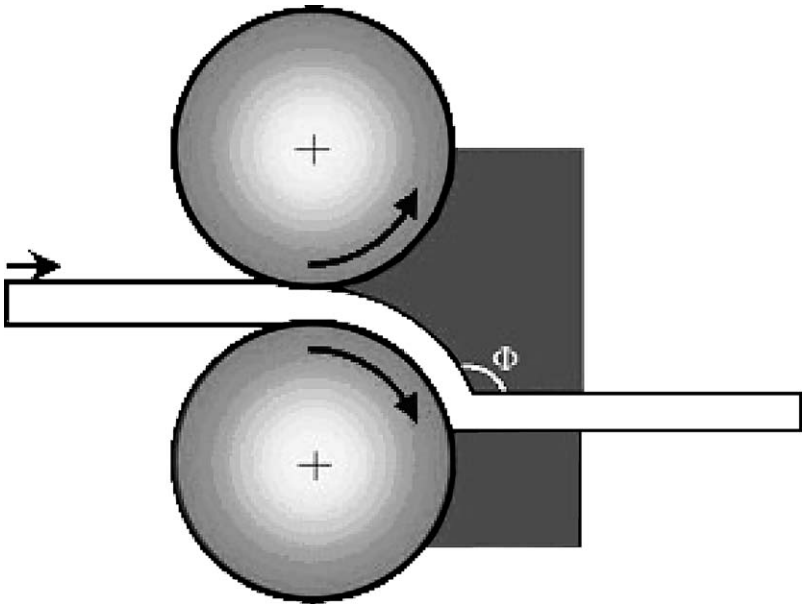

Figure 1 Schematic diagram of the CCSS process.

rolls of ∼10 mm/s. The CCSS deformation was performed in up to three passes; between the passes, the loading direction of samples was maintained. Finally, the deformed sheets recrystallization annealed for 1 h at 700°C in a salt bath.

Pole figure measurements were carried out by means of a conventional X-ray texture goniometer [8]. From three incomplete pole figures, the three-dimensional orientation distribution functions (ODF) $f(g)$ were calculated by the series expansion method according to Bunge ($l_{\max} = 22$) [9]. The ODFs were calculated in the Euler angle range $\{0° \leq \varphi_1 \leq 180°, 0° \leq \Phi, \varphi_2 \leq 90°\}$. For microstructural characterization optical microscopy, electron backscattered diffraction (EBSD) and transmission electron microscopy (TEM) were employed.

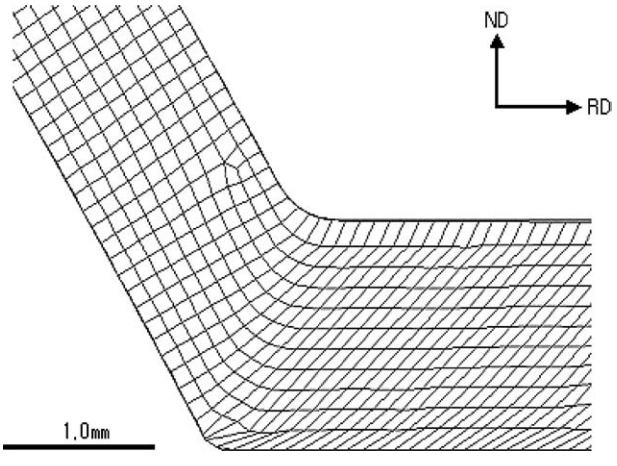

Figure 2 Two-dimensional FEM simulation showing shear deformation during CCSS.

3. Results and discussion

The strain history during CCSS was simulated by means of the rigid-plastic finite element method (FEM) code DEFORM*. The FEM simulation in Fig. 2 shows the overall deformation in the die channel during one pass of CCSS. Changes of the shape of the FEM elements indicate that the shear deformation is not homogeneous through the sheet thickness, in particular at the sheet surface. However, close to the center layer of the strip quite uniform shear deformation prevails. Accordingly, hereafter the analysis of texture and microstructure during CCSS is focused on the sheet center. The integral shear strain derived from the FEM simulations amounts to $\varepsilon_{13} = 0.5$, which is consistent with the shear angle of 45° in Fig. 2.

The {110} pole figures as obtained by conventional X-ray diffraction techniques show the variation of textures in this experiment (Fig. 3). As mentioned previously, the as-received material was cold rolled and fully recrystallized IF steel sheet. The initial sample displayed pronounced {111}//ND orientations (Fig. 3a). Fig. 3b shows an example of the {110} pole figures of the IF steel strips deformed by CCSS. After the CCSS process, pronounced {110} poles developed at the position 20° away from ND. It was noted that the type and intensity of textures hardly changed with increasing number of CCSS passages. Again, the deformation texture was strongly preserved after recrystallization annealing at 700°C for 1 h (Fig. 3c).

In order to investigate the evolution of CCSS textures more precisely, ODFs $f(g)$ were calculated by the series expansion method ($l_{\max} = 22$) [9]. Because pole

TABLE I Orientation stability calculated under imposed shear deformation of $\varepsilon_{13} = 0.5$

Orientation	ω_{RD}	ω_{TD}	ω_{ND}
{122}⟨621⟩	0.00	0.04	0.01
{111}⟨112⟩, {111}⟨110⟩	0.00	0.50	0.00
{125}⟨121⟩	0.02	−0.11	0.46

*DEFORM is a registered trademark of Scientific Forming Technologies Corporation, Columbus, OH.

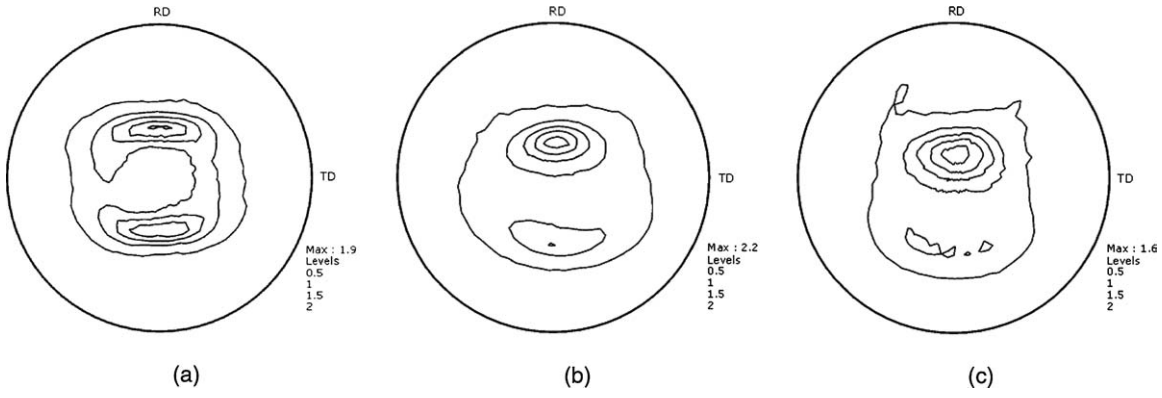

Figure 3 {110} pole figures measured from (a) initial sample, (b) sample after three passages of CCSS and (c) sample after recrystallization anneal.

figures in Fig. 3 do not display the orthotropic symmetry characteristic of most rolled sheets after the CCSS deformation and recrystallization, ODFs were calculated under the assumption of monoclinic sample symmetry and presented in the Euler space with size $\{0^\circ \leq \varphi_1 \leq 180^\circ, 0^\circ \leq \Phi, \varphi_2 \leq 90^\circ\}$.

ODFs in Fig. 4 show the textures after three passages of CCSS and subsequent recrystallization annealing. Pronounced γ-fiber orientations of the initial IF steel sheet were quite unstable under the strain state of the CCSS process. After the first pass of CCSS, γ-fiber orientations of the initial sample drastically vanished and the texture maximum found at orientations with Euler angles (165°, 50°, 25°) and (24°, 50°, 65°) and the approximate Miller-indices $(122)[\bar{6}21]$ and $(211)[2\bar{6}1]$. It seems that $\{122\}\langle 621\rangle$ is stable under the strain state of CCSS since preferred orientations close to $\{122\}\langle 621\rangle$ persisted during further CCSS passages.

The stability of orientations under imposed strain states can be examined by Taylor type deformation model [10]. FEM result in Fig. 2 disclosed that the deformation by CCSS process is simplified by the shear deformation of $\varepsilon_{13} = 0.5$. In order to examine the stability of $\{122\}\langle 621\rangle$, $\{111\}\langle 112\rangle$ and $\{111\}\langle 110\rangle$ as the γ-fiber orientations and $\{125\}\langle 121\rangle$ as a random orientation, the rotation angles around RD, TD and ND were calculated for the imposed shear deformation of $\varepsilon_{13} = 0.5$. Here, a smaller rotation angle indicates a higher stability under the imposed strain. Obviously, $\{111\}\langle 110\rangle$ and $\{111\}\langle 112\rangle$ of γ-fiber orientations are quite unstable in shear deformation and are subject to a large rotation around TD. In contrast, $\{122\}\langle 621\rangle$ shows a high stability in all the sample axes. Accordingly, it is concluded that the stability of $\{122\}\langle 621\rangle$ under shear deformation leads to the formation of this texture in IF steel during CCSS. With increasing number of CCSS passages, the intensity of the shear texture component $\{122\}\langle 621\rangle$ is hardly increased. Dislocation slip accompanying the plastic deformation gives rise to the crystallographic rotation of grains to one of stable orientations and thus leads to the development of deformation texture components. However, the present result implies that other deformation mechanisms may act during CCSS.

Upon recrystallization annealing at 700°C for 1 h, the texture remained nearly unchanged (Fig. 4b). In cold rolled IF steel sheets, recrystallization annealing leads to the formation of the characteristic {111}//ND γ-fiber recrystallization textures. Both preferred nucleation at grain boundaries and growth selection leads to the evolution of the recrystallization textures in IF steels, e.g. [7, 11]. Unlike the cold rolled IF steel, operation of these mechanisms seems to be improbable since the recrystallization texture inherited its deformation texture.

TEM observations revealed a highly work hardened microstructure after CCSS typical of ECAP processes. Similar to ECAP deformation routes, analysis of selected area diffraction patterns (SAD) revealed that the degree of misorientations within the deformed grains increased with increasing number of CCSS passages.

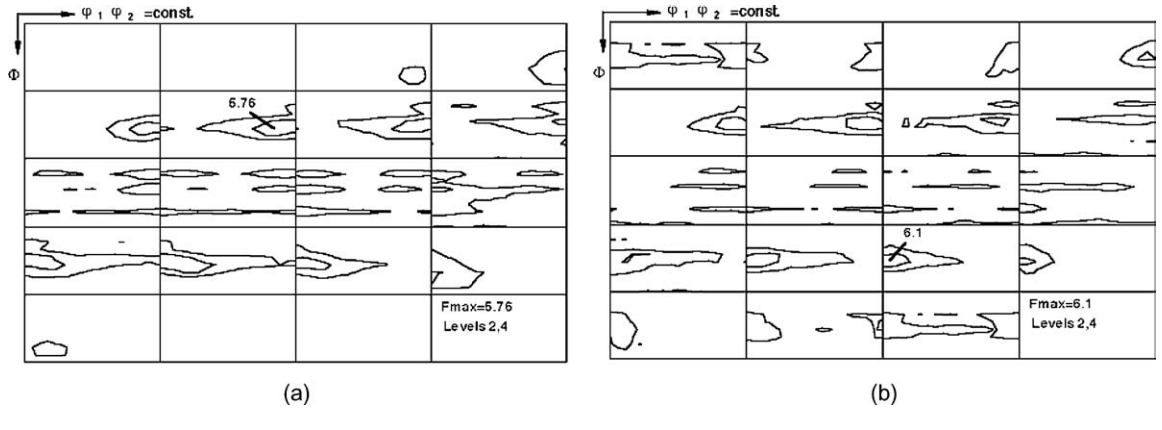

Figure 4 ODFs (a) after three passages of CCSS and (b) after recrystallization anneal.

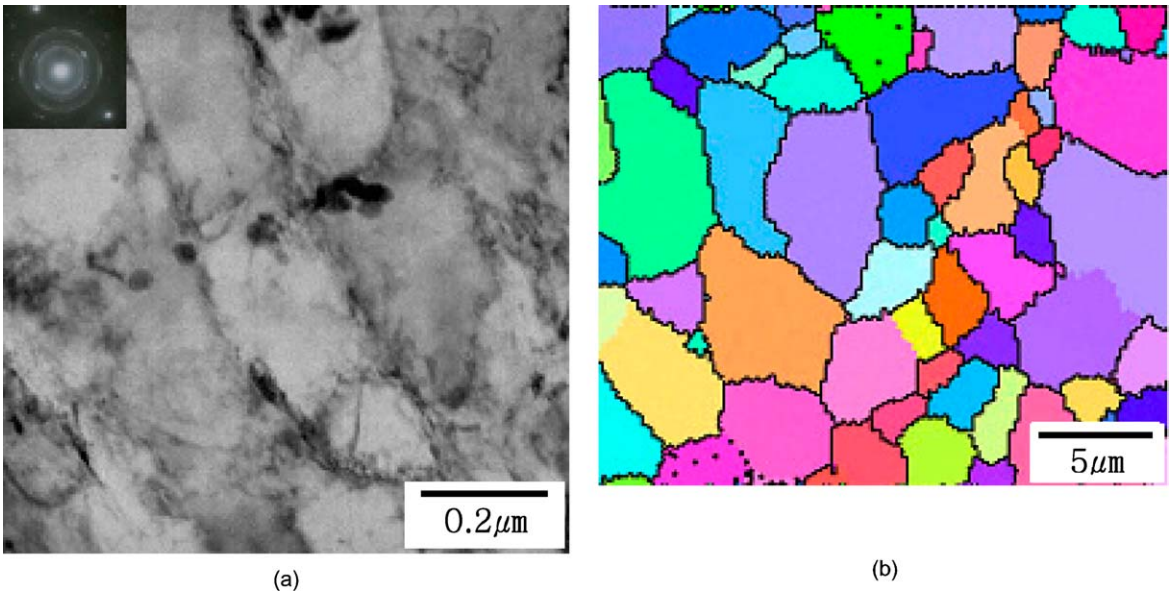

Figure 5 (a) TEM microstructure after three passages of CCSS. (b) EBSD after recrystallization anneal.

Fig. 5a shows the evolution of very small elongated grains of ~300 nm after three passes CCSS. Although the boundaries between these grains were not sharply defined, selected area diffraction pattern frequently revealed high-angle grain boundaries with misorientations larger than 15°. After recrystallization annealing, the samples deformed by CCSS comprised very small grains less than 2.0 μm. Quantitative analysis of the EBSD in Fig. 5b provides an average grain size of 2.3 μm and an average misorientation in excess of 30°.

As addressed above, the IF steel deformed by CCSS displayed the recrystallization texture similar to the deformation texture and very small recrystallized grains. Nucleation at distinct orientations and their selective growth give rise to the evolution of strong texture components and consequently lead to the formation of large recrystallized grains. However, it seems that these processes can be suppressed in highly deformed microstructure formed after repeated shear deformation.

4. Summary

IF steel sheets were deformed by CCSS based on the ECAP. The CCSS process led to the formation of the component of {122}⟨621⟩ which possesses a orientation stability under the imposed shear strain. The intensity of shear deformation texture was hardly increased with increasing number of CCSS passages. In samples processed by CCSS, the preferred nucleation and selective growth were suppressed in highly deformed microstructure and consequently led to the evolution of the recrystallization texture similar to the deformation texture and the formation of small recrystallized grains.

Acknowledgements

This work was supported by Center for Nanostructured Materials Technology.

References

1. R. Z. VALIEV, N. A. KRASILNIKOV and N. K. TSENEV, *Mater. Sci. Eng.* A **137** (1991) 35.
2. D. H. SHIN, I. KIM, J. KIM, Y. S. KIM and S. L. SEMIATIN, *Acta Mater.* **51** (2003) 983.
3. J. C. LEE, H. K. SEOK, J. H. HAN and Y. H. CHUNG, *Mater. Res. Bull.* **36** (2001) 997.
4. Y. H. CHUNG, J. P. AHN, H. D. KIM, B. B. HWANG, O. ENGLER and M. Y. HUH, *Mater. Sci. Forum* **408–412** (2002) 1495.
5. J. C. LEE, H. J. SEOK and J. Y. SUH, *Acta Mater.* **50** (2002) 4005.
6. Y. H. CHUNG, H. D. KIM, H. T. JEONG, O. ENGLER and M. Y. HUH, *Mater. Sci. Forum* **396–402** (2002) 475.
7. M. Y. HUH, Y. S. CHO, J. S. KIM and O. ENGLER, *Z. Metallkd.* **90** (1999) 124.
8. V. RANDLE and O. ENGLER, "Introduction to Texture Analysis, Macrotexture, Microtexture and Orientation Mapping" (Gordon and Breach, Amsterdam, 2000).
9. H. J. BUNGE, "Texture Analysis in Materials Science" (Butterworths, London, 1982).
10. G. I. TAYLOR, *J. Inst. Metall.* **62** (1938) 307.
11. E. J. SHIN, B. S. SEONG, C. H. LEE, H. J. KANG and M. Y. HUH, *Steel Research* **74** (2003) 356.

Received 11 September 2003
and accepted 27 February 2004